Radial glia cells are candidate stem cells of ependymoma

Michael D. Taylor,[1,8] Helen Poppleton,[1,8] Christine Fuller,[2] Xiaoping Su,[3] Yongxing Liu,[3] Patricia Jensen,[1] Susan Magdaleno,[1] James Dalton,[2] Christopher Calabrese,[1] Julian Board,[1] Tobey MacDonald,[4] Jim Rutka,[5] Abhijit Guha,[6] Amar Gajjar,[7] Tom Curran,[1] and Richard J. Gilbertson[1,7,*]

[1]Department of Developmental Neurobiology, St. Jude Children's Research Hospital, 332 North Lauderdale Street, Memphis, Tennessee 38105
[2]Department of Pathology, St. Jude Children's Research Hospital, 332 North Lauderdale Street, Memphis, Tennessee 38105
[3]Hartwell Center for Bioinformatics and Biotechnology, St. Jude Children's Research Hospital, 332 North Lauderdale Street, Memphis, Tennessee 38105
[4]Department of Pediatric Hematology and Oncology, Children's National Medical Center, Washington, D.C. 20010
[5]Division of Neurosurgery and the Arthur and Sonia Labatt Brain Tumor Research Center, Hospital for Sick Children, Toronto, Ontario M5G 1X8, Canada
[6]Division of Neurosurgery, Toronto Western Hospital, Toronto, Ontario M5T 2S8, Canada
[7]Department of Hematology/Oncology, St. Jude Children's Research Hospital, Memphis, Tennessee 38105
[8]These authors contributed equally to this work.
*Correspondence: richard.gilbertson@stjude.org

Summary

Tumors of the same histologic type often comprise clinically and molecularly distinct subgroups; however, the etiology of these subgroups is unknown. Here, we report that histologically identical, but genetically distinct, ependymomas exhibit patterns of gene expression that recapitulate those of radial glia cells in the corresponding region of the central nervous system. Cancer stem cells isolated from ependymomas displayed a radial glia phenotype and formed tumors when orthotopically transplanted in mice. These findings identify restricted populations of radial glia cells as candidate stem cells of the different subgroups of ependymoma, and they support a general hypothesis that subgroups of the same histologic tumor type are generated by different populations of progenitor cells in the tissues of origin.

Introduction

Historically, the diagnosis and treatment of cancer have been based primarily on tumor histology. However, this approach has proven inadequate, as morphologically similar cancers often display variable clinical behavior. Recently, genome-wide expression profiling has unmasked molecularly distinct subgroups among tumors of the same histological type (Nutt et al., 2003; Sotiriou et al., 2003; Yeoh et al., 2002). While these data provide insights into the complexities of human cancer, the etiology of the cancer subgroups remains to be determined.

Recent evidence suggests that cancers arise as the consequence of aberrant development in which the bulk of the malignant cells are maintained by a rare fraction of transformed stem cells, termed cancer stem cells (Pardal et al., 2003; Warner et al., 2004). Cancer stem cells are phenotypically similar to the normal stem cells of the corresponding tissue of origin, but they exhibit dysfunctional patterns of self-renewal and differentiation (Bonnet and Dick, 1997; Hemmati et al., 2003; Ignatova et al., 2002; Lapidot et al., 1994; Singh et al., 2004b). For example, astrocytic and embryonal brain tumors contain rare populations of cancer stem cells that are capable of self-renewal in vitro and of propagating the original tumor in vivo (Hemmati et al., 2003; Ignatova et al., 2002; Singh et al., 2003, 2004b; Yuan et al., 2004). These stem cell-like properties are restricted to brain tumor cells that express the neural stem cell marker CD133 (Uchida et al., 2000).

If cancers arise from transformed stem cells, then subgroups of the same histologic tumor type might be derived from distinct populations of progenitor cells in the tissue of origin. Indeed, recent studies indicate that clinically and molecularly distinct subgroups of acute lymphoblastic leukemia originate at different stages of the hematopoietic lineage (Castor et al., 2005). Comparative studies of normal and malignant hematologic stem cells have been facilitated by the availability of robust assays for all stages of hematopoiesis (Warner et al., 2004). In contrast, knowledge of the stem and progenitor cell populations

SIGNIFICANCE

The failure of tumor histology to accurately predict the clinical behavior of human cancer presents a fundamental hurdle to the development of effective treatments for malignant disease. We present evidence that histologically identical subsets of ependymoma arise from distinct populations of progenitor cells in the nervous system. Our data suggest a mechanism to explain clinical heterogeneity among microscopically similar cancers. Cancer treatments should be targeted to the cell signal pathways that maintain subsets of cancer stem cells rather than the histological or clinical forms of the disease.

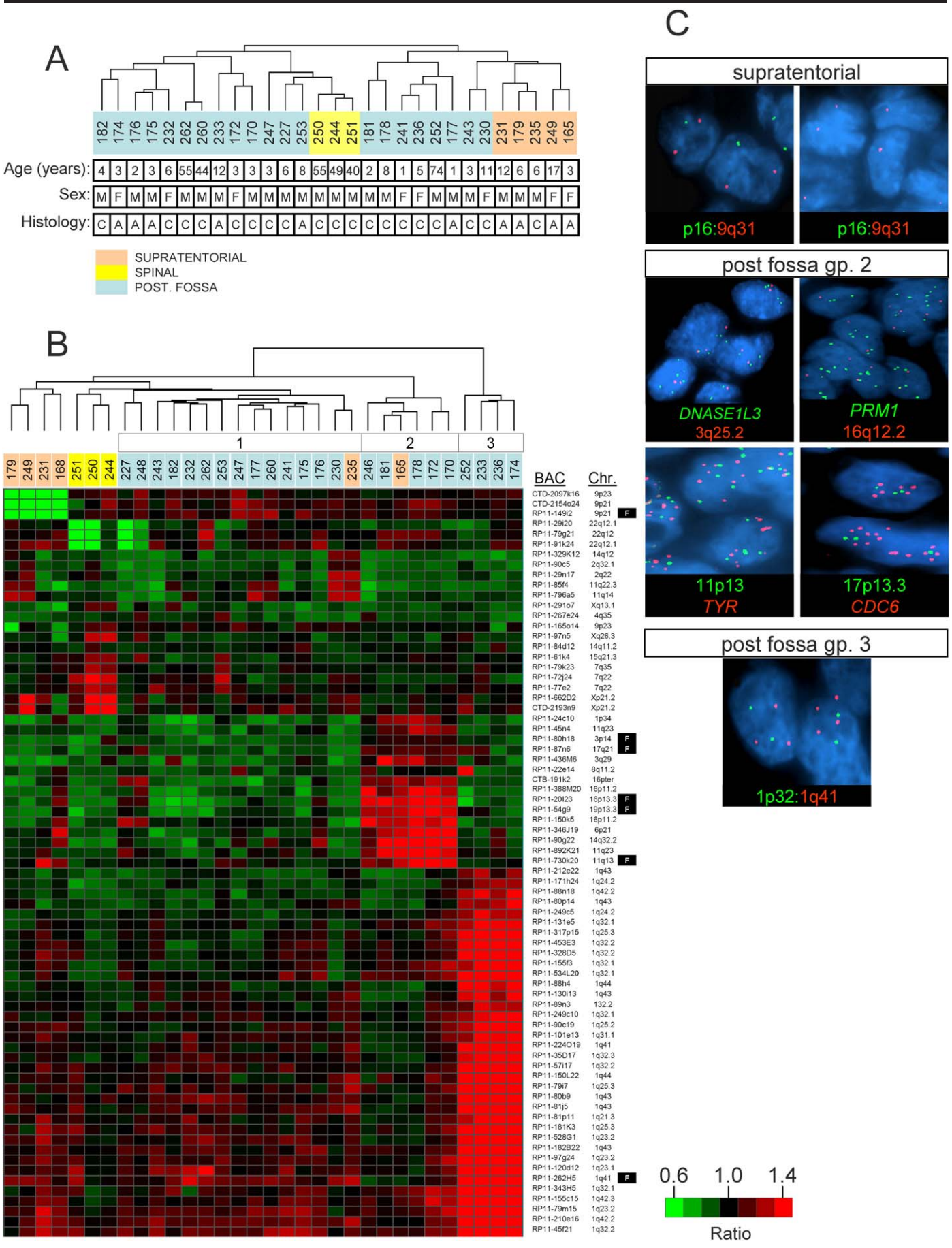
A
182 174 176 175 232 262 260 233 172 170 247 227 253 250 244 251 181 178 241 236 252 177 243 230 231 179 235 249 165
Age (years): 4 3 2 3 6 55 44 12 3 3 3 6 8 55 49 40 2 8 1 5 74 1 3 11 12 6 6 17 3
Sex: M F M M F M M M F M M M M M M M M F F M M M F M M M F F
Histology: C A A A C C C A C C C C A C C C C C C C C A C C A A C A A
SUPRATENTORIAL
SPINAL
POST. FOSSA
B
1
2
3
179 249 231 168 251 250 244 227 248 243 182 232 262 253 247 177 260 241 175 176 230 235 246 181 165 178 172 170 252 233 236 174
BAC Chr.
CTD-2097k16 9p23
CTD-2154o24 9p21
RP11-149i2 9p21 F
RP11-29i20 22q12.1
RP11-79g21 22q12
RP11-91k24 22q12.1
RP11-329K12 14q12
RP11-90c5 2q32.1
RP11-29n17 2q22
RP11-85f4 11q22.3
RP11-796a5 11q14
RP11-291o7 Xq13.1
RP11-267e24 4q35
RP11-165o14 9p23
RP11-97n5 Xq26.3
RP11-84d12 14q11.2
RP11-61k4 15q21.3
RP11-79k23 7q35
RP11-72j24 7q22
RP11-77e2 7q22
RP11-662D2 Xp21.2
CTD-2193n9 Xp21.2
RP11-24c10 1p34
RP11-45n4 11q23
RP11-80h18 3p14 F
RP11-87n6 17q21 F
RP11-436M6 3q29
RP11-22e14 8q11.2
CTB-191k2 16pter
RP11-388M20 16p11.2
RP11-20i23 16p13.3 F
RP11-54g9 19p13.3 F
RP11-150k5 16p11.2
RP11-346J19 6p21
RP11-90g22 14q32.2
RP11-892K21 11q23
RP11-730k20 11q13 F
RP11-212e22 1q43
RP11-171h24 1q24.2
RP11-88n18 1q42.2
RP11-80p14 1q43
RP11-249c5 1q24.2
RP11-131e5 1q32.1
RP11-317p15 1q25.3
RP11-453E3 1q32.2
RP11-328D5 1q32.2
RP11-155f3 1q32.1
RP11-534L20 1q32.1
RP11-88h4 1q44
RP11-130i13 1q43
RP11-89n3 132.2
RP11-249c10 1q32.1
RP11-90c19 1q25.2
RP11-101e13 1q31.1
RP11-224O19 1q41
RP11-35D17 1q32.3
RP11-57i17 1q32.2
RP11-150L22 1q44
RP11-79i7 1q25.3
RP11-80b9 1q43
RP11-81j5 1q43
RP11-81p11 1q21.3
RP11-181K3 1q25.3
RP11-528G1 1q23.2
RP11-182B22 1q43
RP11-97g24 1q23.2
RP11-120d12 1q23.1
RP11-262H5 1q41 F
RP11-343H5 1q32.1
RP11-155c15 1q42.3
RP11-79m15 1q23.2
RP11-210e16 1q42.2
RP11-45f21 1q32.2
0.6 1.0 1.4
Ratio
C
supratentorial
p16:9q31
p16:9q31
post fossa gp. 2
DNASE1L3
3q25.2
PRM1
16q12.2
11p13
TYR
17p13.3
CDC6
post fossa gp. 3
1p32:1q41

of nonhematologic organs is limited; therefore, determining whether different progenitors might generate subtypes of histologically similar solid tumors is less straightforward. Nevertheless, the central nervous system (CNS) represents an attractive system in which to study this hypothesis, since it comprises a set of anatomically and developmentally distinct tissue compartments that are each affected by a common set of tumors.

Ependymomas are CNS tumors that originate from the wall of the ventricular system along the entire craniospinal axis (Kleihues et al., 2002). Although ependymomas from different regions of the CNS are histologically indistinguishable, they display distinct patterns of clinical behavior (Bouffet et al., 1998) and chromosomal abnormalities (Dyer et al., 2002; Ebert et al., 1999), suggesting that they represent a collection of different diseases. We hypothesized that ependymomas from the supratentorial region, the posterior fossa (fourth ventricle), and the spinal cord are clinically heterogeneous because they arise from different populations of neural progenitor cells. We show that the gene expression profiles of human supratentorial and spinal ependymomas are shared by murine embryonic radial glia cells (RGCs) in the subventricular zone of the lateral ventricles and spinal canal, respectively. Further, we demonstrate that ependymomas contain a rare population of RGC-like cancer stem cells that are both required and sufficient to propagate the disease as orthotopic transplants in mice. In addition, we found that ependymomas arising from different parts of the CNS contain distinct chromosomal abnormalities that also contribute to the gene expression signatures of these tumors. Thus, our data identify restricted populations of RGCs as candidate cells of origin of the different anatomic subgroups of ependymomas. Furthermore, the experimental approach that we have used could be employed to identify cellular targets of primary mutations and malignant transformation in other solid tumors.

Results

Ependymomas from different parts of the CNS are molecularly distinct diseases

We used a combination of oligonucleotide gene expression arrays and array comparative genomic hybridization (aCGH) to determine the degree to which ependymomas from different regions of the CNS are molecularly distinct diseases. We analyzed a total of 103 ependymomas, including 32 fresh-frozen tumors and a nonoverlapping set of 71 formalin-fixed tumors that were incorporated into a tissue microarray (TMA). We found that subsets of ependymoma exhibited distinct patterns of gene expression (Figure 1A) and regions of chromosome gain and loss (Figure 1B) that correlated with the anatomic location of the tumor (supratentorial region, posterior fossa, or spine), but not with clinical parameters (patient age or sex) or with tumor histologic grade (classic or anaplastic). Fluorescence in situ hybridization (FISH) analysis of our ependymoma TMA validated the results of our aCGH experiment (Figures 1B and 1C). In this regard, we confirmed that *P16^{INK4A}* (located at 9p21.3) is selectively deleted in >90% of tumor cell nuclei of supratentorial ependymomas but is rarely deleted in tumors arising in other regions of the CNS ($p < 0.0001$). Three subgroups of posterior fossa ependymoma that were identified by aCGH were also confirmed using FISH analysis (Figures 1B and 1C). These included a set of tumors that contained multiple concurrent DNA amplifications, and a further set of tumors that gained chromosome 1q (Figure 1C). In agreement with the results of chromosome CGH studies, around one-half of posterior fossa ependymomas exhibited a balanced karyotype (Dyer et al., 2002). Deletions of chromosome 22q12 that we detected in two spinal ependymomas and one posterior fossa ependymoma are a well-described feature of this disease (Ebert et al., 1999; Huang et al., 2002; Suarez-Merino et al., 2005). Thus, morphologically similar ependymomas that arise within different regions of the CNS are molecularly distinct diseases.

Ependymomas recapitulate the gene expression profiles of regionally specified RGCs

The gene expression signatures that distinguished supratentorial, posterior fossa, and spinal ependymomas include genes that regulate neural precursor cell proliferation and differentiation in the corresponding region of the CNS (Figure 2A; see Table S1 in the Supplemental Data available with this article online for a full list of genes). For example, supratentorial tumors express markedly elevated levels of members of the EPHB-EPHRIN and NOTCH cell signal systems that play key roles in maintaining normal neural stem cells in the cerebral SVZ (Conover et al., 2000; Hitoshi et al., 2002) (Figure 2A). Interference with normal EphB-Ephrin interactions in SVZ cells of mice disrupts neuroblast chain migration and dramatically increases astrocyte proliferation, resulting in the formation of hyperplastic polyps along the ventricle surface (Conover et al., 2000). Conversely, spinal ependymomas expressed multiple Homeobox (*HOX*) family members (Figure 2A). *HOX* genes encode transcription factors that coordinate anteroposterior tissue patterning during development (Dasen et al., 2003; Kmita and Duboule, 2003). In vertebrates, successively more caudal body regions show an increase in the amount and diversity of *HOX* expression, and deletion of either *Hoxa9* (Fromental-Ramain et al., 1996) or *Hox-c* (Suemori and Noguchi, 2000),

Figure 1. Ependymomas from different parts of the CNS are molecularly distinct diseases

Unsupervised hierarchical cluster analyses of gene expression profiles of 29 ependymomas (histologic variants are classic ["C"] and anaplastic ["A"]) (**A**) and aCGH data sets of the same 29 tumor samples plus one additional supratentorial and two posterior fossa tumors (**B**). Tumor color codes are the same as in **A**. Reference numbers of the bacterial artificial chromosome (BAC) clones that reported significantly altered chromosome (Chr) regions are shown to the right. In **B**, black boxes denoted "F" identify BAC clones that were employed for fluorescence in situ hybridization (FISH) analysis of our TMA, the results of which are shown in **C**. Three separate subgroups (1–3) of posterior fossa tumors are identified by aCGH. Group 1 has a balanced karyotype, group 2 has a collection of amplifications on various autosomes, and group 3 shows amplification of chromosome 1q. **C:** Confirmation of aCGH data by FISH analysis of our ependymoma TMA. Heterozygous or homozygous deletions of *p16* were detected in four of six supratentorial tumors but in only 1 of 69 other informative ependymomas (Fisher's test, $p < 0.0001$). Multiple, concurrent, nonrandom DNA amplifications were detected in eight posterior fossa tumors (group 2), which were distinct from tumors that demonstrated gain of 1q (group 3).

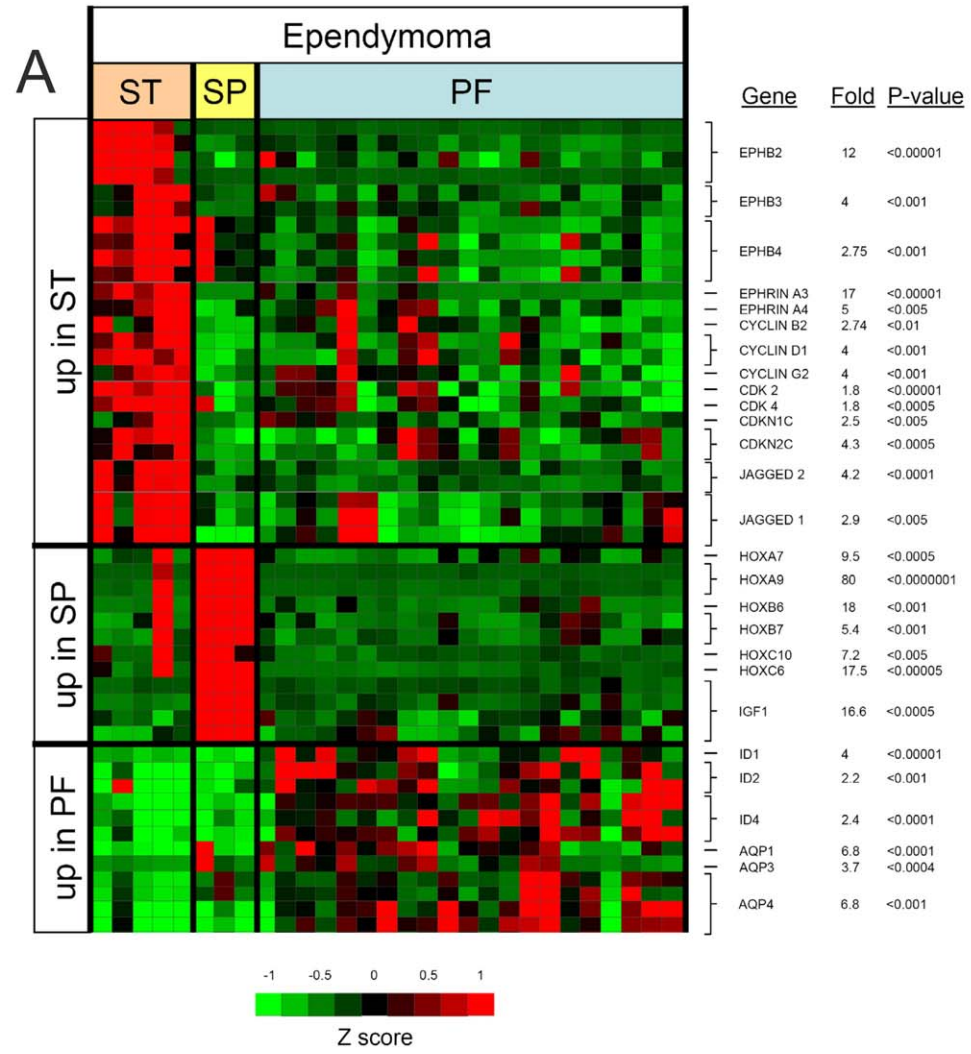
A
Ependymoma
ST
SP
PF
up in ST
up in SP
up in PF
Gene Fold P-value
EPHB2 12 <0.00001
EPHB3 4 <0.001
EPHB4 2.75 <0.001
EPHRIN A3 17 <0.00001
EPHRIN A4 5 <0.005
CYCLIN B2 2.74 <0.01
CYCLIN D1 4 <0.001
CYCLIN G2 4 <0.001
CDK 2 1.8 <0.00001
CDK 4 1.8 <0.0005
CDKN1C 2.5 <0.005
CDKN2C 4.3 <0.0005
JAGGED 2 4.2 <0.0001
JAGGED 1 2.9 <0.005
HOXA7 9.5 <0.0005
HOXA9 80 <0.0000001
HOXB6 18 <0.001
HOXB7 5.4 <0.001
HOXC10 7.2 <0.005
HOXC6 17.5 <0.00005
IGF1 16.6 <0.0005
ID1 4 <0.00001
ID2 2.2 <0.001
ID4 2.4 <0.0001
AQP1 6.8 <0.0001
AQP3 3.7 <0.0004
AQP4 6.8 <0.001
-1 -0.5 0 0.5 1
Z score

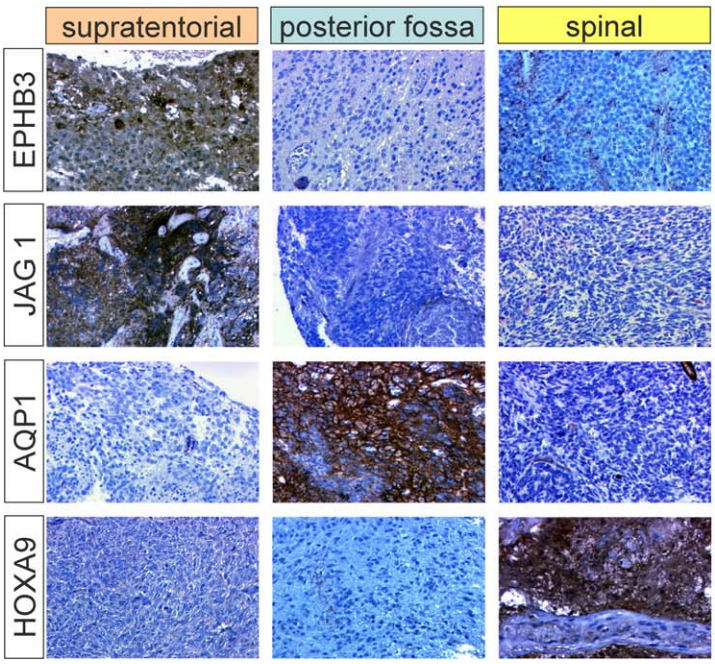
B
supratentorial
posterior fossa
spinal
EPHB3
JAG 1
AQP1
HOXA9

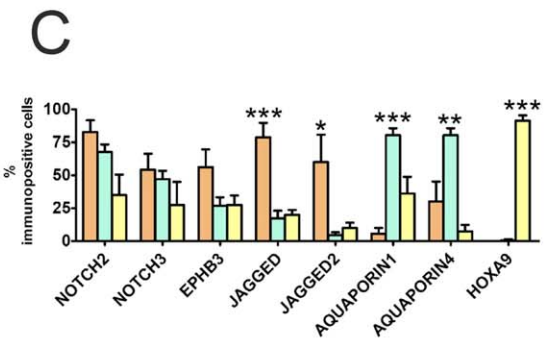
C
% immunopositive cells
100
75
50
25
0
***
*
***
**
***
NOTCH2
NOTCH3
EPHB3
JAGGED
JAGGED2
AQUAPORIN1
AQUAPORIN4
HOXA9

which are selectively expressed by human spinal ependymomas (Figure 2A), causes spinal abnormalities in mice. We confirmed these gene expression patterns by performing immunohistochemical analyses of our ependymoma TMA (Figures 2B and 2C). Importantly, because FISH analysis showed that the great majority of ependymoma cells within our TMA are cancer cells (Figure 1C), these immunohistochemical data also confirm that ependymoma gene expression patterns are generated by cancer cells and not by entrapped normal cells.

Previously, molecular signatures of cancers derived from gene expression microarray studies have been linked to the presence of specific mutations in tumor subtypes (Aguirre et al., 2004); however, our data suggest a different interpretation. Alternatively, it is possible that subsets of ependymoma either maintain or recapitulate the developmental expression profiles of anatomically restricted progenitor cells. Thus, mapping the site of expression of these genes might pinpoint the normal cell populations from which ependymomas arise. Therefore, using in situ hybridization, we mapped the expression in embryonic mouse CNS of 77 genes that clearly distinguished supratentorial, posterior fossa, and spinal ependymomas (see Table S2 for a full list of genes). Almost all signature genes of human supratentorial ependymomas were expressed in the wall of the cerebral ventricles at embryonic day 11 (E11), and in the ventral SVZ of the lateral ventricles at E15 (Figures 3A and 3D). However, these genes were rarely expressed in the wall of the fourth ventricle or in the spinal cord. Conversely, all of the signature genes of spinal ependymoma were expressed in the wall of the developing spinal canal and the ventrolateral spinal cord, whereas less than one-third was present in the brain (Figures 3C and 3D). The gene expression signatures of supratentorial and spinal ependymomas correlated significantly with those of the corresponding region of the normal developing CNS at E11 and E15 (Figure 3D; $p < 0.05$). Although cells lining the fourth ventricle contained transcripts of proportionately more signature genes of human posterior fossa ependymoma, these genes were also expressed in the wall of the lateral ventricles and the spinal canal (Figures 3B and 3D).

Interestingly, the intense expression of supratentorial ependymoma signature genes that we observed in the ventral wall of the lateral ventricle between E11 and E15 coincides precisely with the time that normal ependymal cells arise from RGCs in this region of the brain (Spassky et al., 2005). RGCs constitute a heterogeneous population of multipotent neural precursor cells that display significant differences in gene expression and function among CNS regions (Hartfuss et al., 2001; Kriegstein and Gotz, 2003; McMahon and McDermott, 2002; Russo et al., 2004). Therefore, we reasoned that RGCs might represent the site of expression of ependymoma signature genes in the supratentorial SVZ and spinal canal and that they could be cells of origin of these ependymoma subtypes. To test this hypothesis, we used coimmunofluorescence to colocalize RGC-specific antigens and ependymoma signature genes in the ventral wall of the lateral ventricle and the spinal canal (Figure 3E). These studies confirmed that signature genes of ependymomas are indeed expressed by RGCs in the corresponding region of the CNS and suggest the hypothesis that the distinct populations of RGCs that exist within the brain and spine (Hartfuss et al., 2001; Kriegstein and Gotz, 2003) are the cells of origin of supratentorial and spinal ependymomas, respectively.

Ependymomas contain rare populations of RGC-like cells that self-renew and are multipotent in culture

Normal and malignant neural stem cells may be isolated in culture as clonally derived colonies termed neurospheres (Reynolds and Weiss, 1992). Neurosphere (hereon termed tumor sphere)-forming cells isolated from medulloblastoma and glioma express the neural stem cell marker CD133 and exhibit the ability to self-renew and differentiate along divergent neuronal lines (Hemmati et al., 2003; Ignatova et al., 2002; Singh et al., 2003; Uchida et al., 2000; Yuan et al., 2004). We reasoned that if RGCs are stem cells of ependymoma, then cancer stem cells of this tumor should be capable of self-renewal, be multipotent, and express markers of RGCs.

To test this hypothesis, we generated single-cell suspensions from samples of freshly resected intracranial (n = 4) and spinal pediatric ependymoma (n = 1) and cultured these under conditions that favor stem cell growth. We also confirmed that each of these cell populations comprised tumor cells and not normal brain cells, by performing spectral karyotyping (Table S3). All five ependymomas were found to contain a minority cell population that generated clonally derived tumor spheres at a frequency ranging from 0.34% to 0.74% (Table S3). This frequency of primary tumor sphere-forming cells is very similar to that reported for pilocytic astrocytoma; another relatively slow-growing pediatric brain tumor (Singh et al., 2003).

To assay the self-renewal capacity of ependymoma tumor sphere-forming cells, we dissociated primary tumor spheres and replated single-cell suspensions of these cells at serial dilutions down to one cell per well. Primary tumor sphere-derived cells formed secondary spheres with a range of 0.53 to 1.0 secondary sphere/100 primary sphere cells (mean 0.75 ± 0.22 SE) over a period of 1–2 weeks. Thus, ependymomas contain a rare fraction of cells that self-renew under stem cell culture conditions.

To determine if tumor sphere-forming ependymoma cells might be derived from RGCs, we looked in these cells for marker proteins characteristic of different stages of differentiation in the SVZ. Neuroepithelial cells represent the earliest progenitors in

Figure 2. Regulators of neural stem cell proliferation and differentiation are signature genes of ependymomas from different parts of the CNS

A: Supervised hierarchical cluster analysis of oligonucleotide gene expression profiles of supratentorial (ST), posterior fossa (PF), and spinal (SP) ependymomas. "Fold" and "p value" denote the magnitude and significance of the difference in gene expression among anatomic tumor subgroups.

B: Examples of immunohistochemical analyses of ten supratentorial, 40 posterior fossa, and 21 spinal ependymomas confirming the differential expression between anatomic tumor subgroups of genes detected by gene expression profiling.

C: Differences in the expression of these proteins were quantified by counting the numbers of immunoreactive tumor cells in each tumor. Pink, blue, and yellow bars denote supratentorial, posterior fossa, and spinal tumors, respectively. Each bar reports average (±SE) number of immunoreactive tumor cells. Differences in the expression of proteins among tumor subgroups were determined by the Kruskall-Wallis test; *$p < 0.05$; **$p < 0.005$; ***$p < 0.0005$.

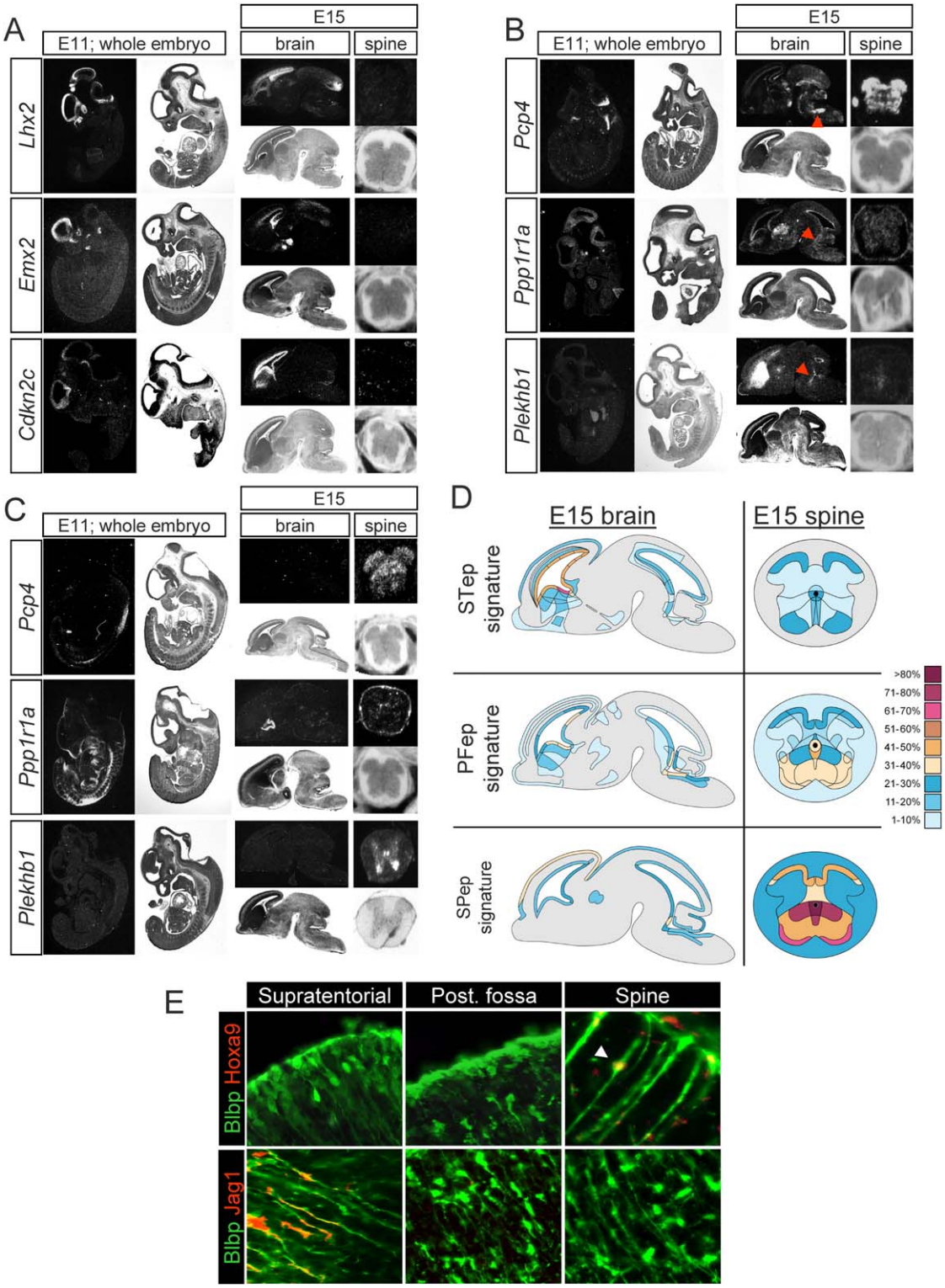

Figure 3. Ependymomas recapitulate the gene expression profiles of regionally specified precursor cells

A–C: In situ hybridization analysis showing expression in E11 whole embryo and E15 mouse brain and spinal cord of signature genes of human supratentorial (**A**), posterior fossa (**B**), and spinal (**C**) ependymoma. Arrows in **B** identify the IV ventricle.

D: Contour map showing the frequency and site of expression in E15 mouse brain and spine of all 77 genes that clearly distinguished human supratentorial (STep), posterior fossa (PFep), and spinal (SPep) ependymomas. Color scale reports the percentage of tumor signature genes expressed (see Table S2 for a full list of genes).

E: Dual immunofluorescence analysis of Jagged1 or Hoxa9 expression by radial glia cells (detected by staining for Blbp) in the wall of the lateral ventricle (supratentorial), IV ventricle (post. fossa), and spinal canal (spine) in E15 mouse CNS. Arrow indicates Hoxa9 expression within the nucleus of a Blbp+ RGC.

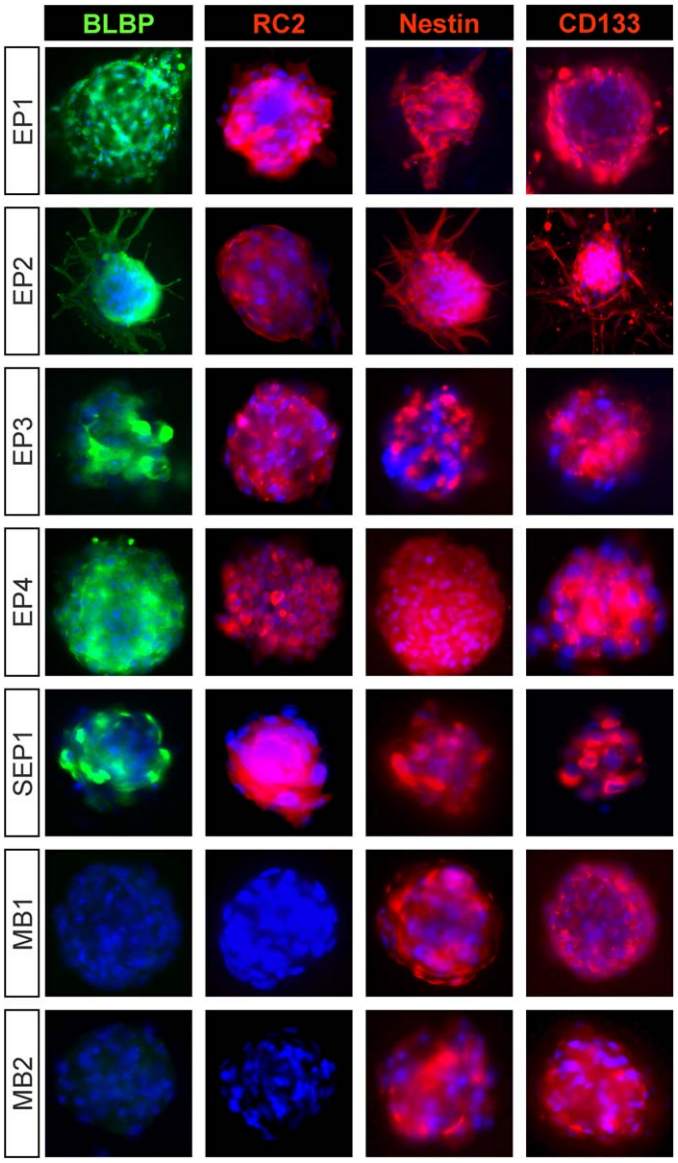

Figure 4. Tumor sphere-forming ependymoma cells display a radial glia cell immunophenotype

Clonally derived secondary tumor spheres generated by ependymoma and medulloblastoma stem cell-like cells after 7 days in culture express the neural progenitor cell markers Nestin and CD133. Only ependymoma spheres expressed RC2 and the radial glia cell marker BLBP.

the CNS; these cells are the immediate precursors of RGCs and they express CD133, Nestin, and RC2 (Hartfuss et al., 2001; Uchida et al., 2000). While RGCs also express these proteins, they are distinguished from neuroepithelial cells by the presence of glial markers including astrocyte-specific glutamate transporter (GLAST) and brain lipid binding protein (BLBP) (Hartfuss et al., 2001; Kriegstein and Gotz, 2003). As neurogenesis begins, RGCs give rise to postmitotic neurons, astrocytes, and ependymal cells expressing appropriate markers of differentiation but not CD133 or Nestin (Culican et al., 1990; Hartfuss et al., 2001; Malatesta et al., 2003; Spassky et al., 2005; Uchida et al., 2000). We found that all ependymoma-derived tumor spheres displayed a CD133+/Nestin+/RC2+/BLBP+ immunophenotype similar to that of RGCs (Figure 4). In contrast, tumor spheres generated from pediatric medulloblastoma exhibited a CD133+/Nestin+/RC2–/BLBP– phenotype. Significantly, analysis of the 71 ependymomas within our TMA also identified BLBP-expressing tumor cells at an average frequency of 0.5% (range 0.001% to 1.5% of total tumor cells). Thus, stem cell-like cancer cells in ependymoma are phenotypically different from those of medulloblastoma, and they are likely to arise within the RGC lineage.

To test whether tumor sphere-forming ependymoma cells are multipotent, we generated single-cell suspensions from secondary tumor spheres and cultured these in the absence of both basic fibroblast growth factor and epidermal growth factor to induce differentiation. Twenty-four hours following dissociation, approximately 70% and 30% of secondary tumor sphere-derived cells retained expression of BLBP and RC2, respectively (Figures 5A–5D). However, a significant number of cells had lost expression of CD133 relative to that observed in the intact tumor spheres (Figures 4, 5A, and 5B). Remarkably, about 1% of secondary tumor sphere-derived cells also displayed an unusual morphology in culture that was reminiscent of RGCs in the brain (Figures 5E and 5F). After 72 hr in differentiation medium, secondary tumor sphere-derived cells exhibited a dramatic change in immunophenotype. These changes included loss of the RGC immunophenotype CD133+/RC2+/BLBP+ (Figures 5A and 5B; and compare Figure 5C with Figure 5G and Figure 5D with Figure 5H) and increased expression of markers of neuronal (β-III-tubulin and MAP2), astrocytic (GFAP and S100), and oligodendrocytic (CNPase and NG2) differentiation (Figures 5I–5N). Importantly, FISH analysis of differentiated ependymoma cells confirmed that these are cancer cells and not normal cells (Figure 5O). Thus, ependymomas contain a rare fraction of RGC-like cancer cells that display the stem cell properties of self-renewal and multipotency.

RGC-like ependymoma cancer stem cells form tumors in nude mice

Although our cell culture assays suggest that ependymomas contain RGC-like cancer stem cells, the ability of a cell to recapitulate the original tumor in vivo is a far more rigorous assessment of the cancer stem cell phenotype. Therefore, we used immunoglobulin-conjugated magnetic beads to isolate CD133+ cells from whole-cell populations of two fresh samples of ependymoma (Figures 6A and 6B). FISH analysis of sorted ependymoma cell populations confirmed that both CD133+ and CD133– fractions comprise cancer cells, since both of these fractions displayed gain of 1q (Figures 6C and 6D). In keeping with our analysis of tumor spheres, acutely sorted CD133+ ependymoma cells coexpressed BLBP and RC2 (Figures 6E and 6F), whereas neither of these proteins were detected in CD133+ cells isolated from medulloblastoma (Figure 6G and data not shown). An average of 0.9% (range 0.3%–3.0%) of all cells within sorted samples of ependymoma displayed a radial glia-like CD133+/RC2+/BLBP+ immunophenotype, which is very similar to the incidence of BLBP+ cells that we observed within whole-tumor sections. We then performed stereotactic injections of sorted and nonsorted tumor cell populations into the superficial cerebral cortex of 7-week-old NOD-SCID mice. Mice injected with as few as 10,000 CD133+/RC2+/BLBP+ ependymoma cells developed signs of neurological impairment

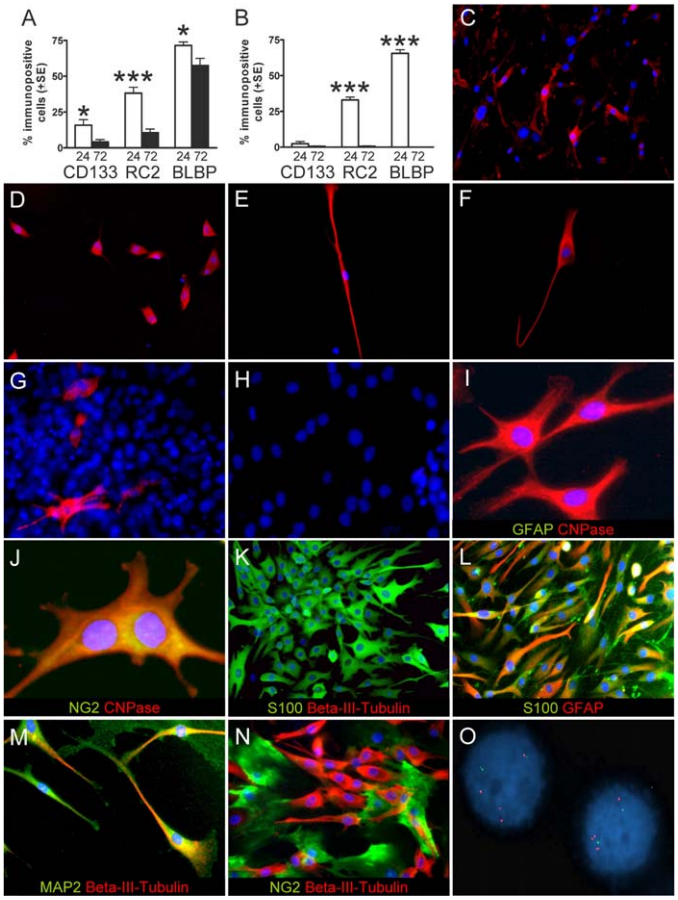

Figure 5. Radial glia cell-like ependymoma cells are multipotent

Single cells isolated from secondary ependymoma tumor spheres were cultured under conditions that induce differentiation. Graphs (**A** and **B**) report changes in the percentage of CD133, RC2, or BLBP expression determined by immunofluorescence among cells isolated from two different primary ependymomas. Percentages (±SE) were estimated by counting >1000 cells after 24 hr and 72 hr in culture. The Wilcoxon statistic was used to estimate the significance of expression differences; *$p < 0.05$; ***$p < 0.0005$. Typical expression patterns of RC2 (**C**) and BLBP (**D**) among ependymoma cells cultured in differentiation medium for 24 hr. **E** and **F** show examples of the 1% of secondary tumor sphere-derived cells (estimated by counting 1000 tumor cells) that displayed a morphology of radial glia cells up to 24 hr in differentiation medium. After 72 hr in differentiation medium, secondary tumor sphere-derived cells exhibited a dramatic decrease in expression of RC2 (**G**) and BLBP (**H**) and a concomitant increase in markers of oligodendrocytic (**I** and **J**), astrocytic (**K** and **L**), and neuronal (**M** and **N**) differentiation. **O:** FISH analysis using probes directed against 1p (green) and 1q (red) confirmed that differentiated cells display gain of 1q and are therefore cancer cells.

between 4 and 5 months postinjection. Analysis of the brains from these mice revealed the presence of tumors that appeared to arise within the cerebral SVZ and fill the lateral or III ventricles, resulting in hydrocephalus (Figure 6H). These xenografts demonstrated characteristic morphologic features of ependymoma including the following: moderate cellularity; predominantly monomorphic nuclear morphology; and occasional pseudorosettes (Figure 6I). CD133+/RC2+/BLBP+ xenografts also expressed glial fibrillary acidic protein and BLBP, but they did not exhibit markers of neuronal differentiation such as β-III-tubulin (Figures 6J–6L). Significantly, xenografts also recapitulated the appropriate site-specific gene expression signature of the parent tumor. In this regard, CD133+/RC2+/BLBP+ cancer stem cells isolated from a posterior fossa ependymoma generated a xenograft that reproduced the gene expression signature of the parent posterior fossa tumor, even when transplanted into the supratentorial region (Figures 6M–6T). In contrast, mice that were injected with up to 2×10^6 CD133– cells or 2×10^6 unsorted ependymoma cells (n = 10 mice for each cell population) did not develop tumors up to 1 year following injection. Histologic examination of the brains of these mice did not reveal any evidence of tumor engraftment. Therefore, ependymomas contain a rare fraction of CD133+/RC2+/BLPB+ cancer stem cells that are required and sufficient to generate tumors in vivo and that transmit a site-specific radial glia-like expression signature to the mature tumor. Thus, we propose that ependymoma cancer stem cells are derived from transformed RGCs.

Anatomic site-specific chromosomal alterations in ependymomas significantly contribute to tumor gene expression profiles

Studies of leukemia suggest that early transformation events, e.g., the t(8;21) translocation, are transmitted from the cancer stem cell to more mature progeny, ultimately impacting the gene expression profile of the entire malignant clone (Castor et al., 2005; Miyamoto et al., 2000; Ross et al., 2004; Yuan et al., 2001). We reasoned that the gene expression signatures of ependymomas might be similarly influenced by the unique sets of chromosomal alterations contained within the different anatomic tumor subgroups (Figure 1B). Further, the genes that are most affected by these chromosome alterations are likely to include those responsible for driving transformation of ependymoma stem cells in the different regions of the CNS.

As a first step to identifying genes that are disrupted by chromosomal alterations in ependymoma, we used a novel statistical approach to integrate our aCGH and gene expression array data sets. We first identified all Affymetrix oligonucleotide probe sets that map within significantly varying bacterial artificial chromosome (BAC) aCGH clones and correlated DNA copy number changes with gene expression using the *t*-like statistic. We then employed random permutation analysis to assess the significance of each statistic for each gene. Importantly, this analysis demonstrated that only a small minority (12%; n = 86/704) of transcripts within regions of DNA gain or loss exhibit significant copy number-driven gene expression (Figure 7; a full list of these genes is provided in Table S4). However, this correlation was highly significant, since only 0.1% (n = 47/40,785) of probes within balanced chromosome regions correlated with the alteration of a distal genomic region (odds ratio = 122; chi-square $p < 0.0001$). This approach may identify the minority of genes in altered genomic regions that contribute to transformation or progression of ependymoma. These findings also imply that transcriptional differences among histologically identical tumors are dictated not only by the cell of origin, but also by the specific genetic events that promote clonal expansion. We are currently mining these data to select genes that display clear copy number-driven gene

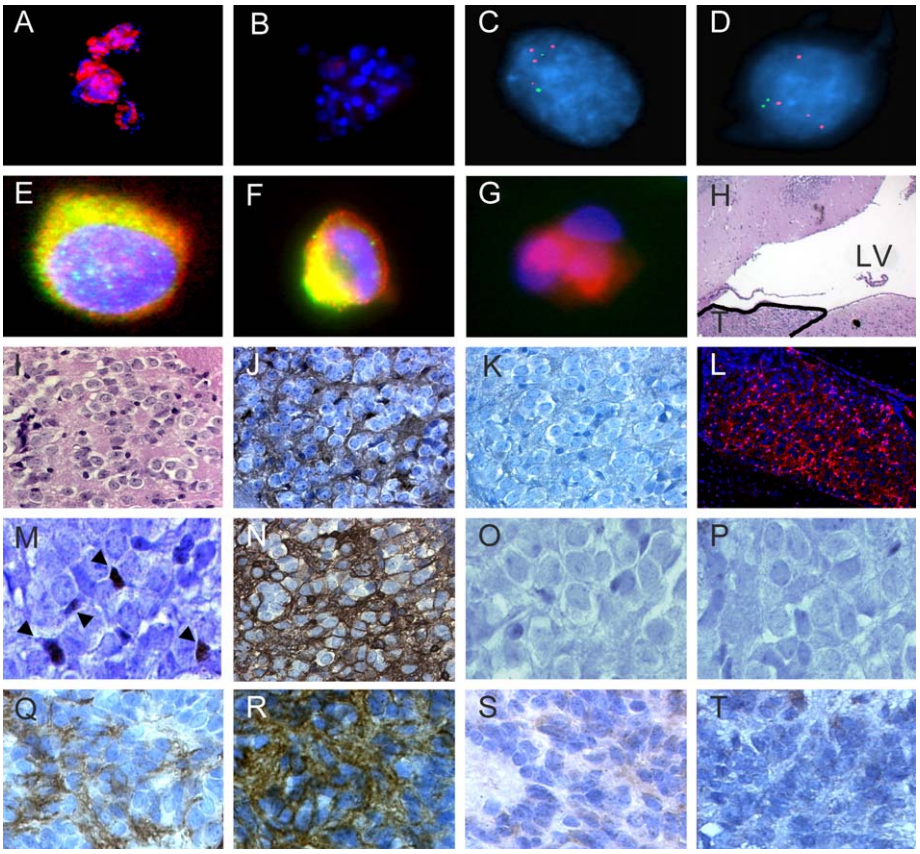

Figure 6. CD133+/RC2+/BLBP+ ependymoma stem cells form tumors in mice

Whole-cell populations of ependymomas were sorted to isolate CD133+/RC2+/BLBP+ cells. Immunofluorescence analysis of CD133 confirmed expression in positively (**A**) but not negatively (**B**) sorted cells. FISH analysis using probes against 1p (green) and 1q (red) confirmed that CD133+ (**C**) and CD133− (**D**) cell fractions display gain of 1q and are therefore cancer cells. Immunofluorescence analysis of acutely sorted ependymoma cells also confirmed that CD133+ cells (red) coexpress BLBP (green) (**E**) and RC2 (green) (**F**). In contrast, CD133 (red)-positive medulloblastoma cells do not express BLBP (green) (**G**). **H:** Tumor (T, outlined) in the lateral ventricle (LV) of a mouse resulting in marked ventricular dilatation. **I:** Hematoxylin and eosin stain of the tumor demonstrating the typical appearance of an ependymoma (×400). Immunohistochemical analysis of GFAP (**J**) and β-III-tubulin (**K**) by an engrafted ependymoma. **L:** Immunofluorescence analysis of BLBP expression (red) by the same ependymoma xenograft. Immunohistochemical analysis of Aquaporin 1 (**M**, arrows indicate immunopositive cells), Aquaporin 4 (**N**), Jagged1 (**O**), and Hoxa9 (**P**) by a xenograft that grew in the lateral ventricle of a mouse and was formed from CD133+/RC2+/BLBP+ stem cells isolated from a posterior fossa tumor. Parallel analysis of Aquaporin 1 (**Q**), Aquaporin 4 (**R**), Jagged1 (**S**), and Hoxa9 (**T**) within the parent posterior fossa tumor confirmed that the xenograft recapitulated the gene expression signature of posterior fossa ependymoma.

expression in ependymoma and are therefore likely to play a role in the etiology of the disease.

Discussion

Are ependymoma cancer stem cells transformed RGCs?

Here, we present several lines of evidence that suggest that histologically similar ependymomas from different parts of the CNS represent molecularly and clinically distinct disease subgroups because they arise from different populations of RGCs. Ependymomas occur most commonly in the wall of the cerebral ventricles or in the spinal canal and they display characteristic ultrastructural and immunohistochemical features of normal ependymal cells (Kleihues et al., 2002; Liberski, 1996). Therefore, these tumors are most likely to arise from cells of the ependymal lineage. Neuroepithelial cells and RGCs, precursors of ependymal cells, are mitotically active (Kriegstein and Gotz, 2003). Thus, both of these cell types could acquire the minimum number of mutations required for malignant transformation. Our data suggest that RGCs, rather than neuroepithelial cells, are stem cells of ependymoma. We show that more than 80% of genes that are expressed at high levels in supratentorial and spinal ependymomas are also present in RGCs in the corresponding region of the embryonic CNS. Furthermore, self-renewing and multipotent cancer cells isolated from ependymomas exhibit the RGC immunophenotype CD133+/Nestin+/RC2+/BLBP+, and they reproduce this disease when transplanted into mice. Currently, we are conducting serial transplantation experiments to confirm that these cells also self-renew in vivo. Although unlikely, we acknowledge that ependymoma cancer stem cells could arise from postmitotic ependymal cells that have reacquired the capacity to self-renew (Capela and Temple, 2002; Laywell et al., 2000; Spassky et al., 2005). Proof of principle that self-renewal can be reestablished has been provided by experiments in which the transduction of hematologic cells with *MOZ-TIF2* restored self-renewal and promoted leukemogenesis (Huntly et al., 2004). In the future, it may be possible to identify precisely which cells in the ependymal lineage are the primary targets of transformation, by using cell-specific promoters to drive oncogene expression in different ependymal precursor populations of transgenic mice.

Which cell signal pathways promote the stem cell phenotype in ependymoma?

An important question raised by our data is whether the gene expression profiles that are hallmarks of the respective RGC populations persist in ependymomas as molecular baggage or whether they play a functional role in maintaining the cancer cell phenotype. Notably, the NOTCH cell signal pathway and HOX family of transcription factors, which we identified as upregulated in supratentorial and spinal ependymomas, respectively, regulate stem cell self-renewal (Huntly and Gilliland, 2005; Pardal et al., 2003). For example, aberrant Notch signaling expands the neural stem cell fraction in the developing mouse and inhibits neurogenesis (Hitoshi et al., 2002). Similarly, exposure of hematologic cell populations to JAGGED1

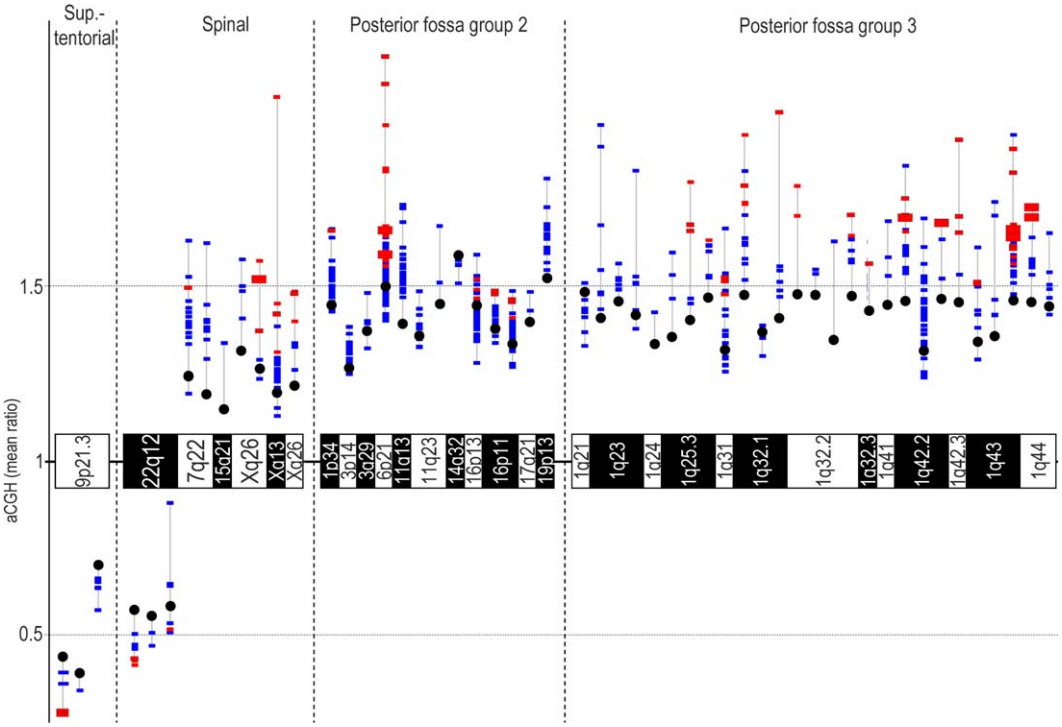

Figure 7. Ependymomas from different parts of the CNS display distinct patterns of copy number-driven gene expression

Solid black circles represent individual DNA regions that were identified as significantly altered in supratentorial (n = 4), spinal (n = 3), posterior fossa group 2 (n = 6), and posterior fossa group 3 (n = 4) ependymomas, by aCGH analysis. The genomic location of each region is shown on the graph. The vertical position of each circle represents the relative average gain (>1 mean aCGH ratio) or deletion (<1 mean aCGH ratio) of each region among tumors in the corresponding disease subgroup. Squares report the relative average expression of genes mapping within the corresponding altered genomic region (see Table S4 for a full list of genes). Squares falling above each circle represent genes that are relatively overexpressed in tumors containing the corresponding genomic alteration: genes that are relatively underexpressed are shown below each circle. The distance of each square from the circle represents the degree to which the gene is under- or overexpressed. Genes that are significantly over- or underexpressed in tumors containing the corresponding DNA alteration are shown in red. Genes displaying nonsignificant expression changes are shown in blue. The size of each square reports the degree of statistical significance of the expression difference.

increases the proportion of stem cells while reducing the numbers of differentiating cells (Varnum-Finney et al., 1998). Interestingly, aberrant NOTCH signaling appears to specifically transform only cells in which the G0/G1 checkpoint is disrupted (Radtke and Raj, 2003). Thus, the markedly elevated levels of JAGGED1 observed in supratentorial ependymomas could contribute to the self-renewal capacity of ependymoma stem cells in the cerebral SVZ. Further, this might be facilitated by deletion of *INK4A/ARF*, which we observed as a frequent event in supratentorial ependymomas. Similarly, aberrant expression of HOXA9 may maintain the cancer stem cell phenotype in spinal ependymomas, since increased expression of this transcription factor has been shown to transform hematologic stem cells and promote leukemogenesis (Huntly and Gilliland, 2005).

Implications for the clinic

Our data complement and extend previous studies of medulloblastoma and glioma indicating that brain tumors are propagated by small fractions of tumorigenic stem cells (Singh et al., 2004a). If proved correct, then these findings would lead to a paradigm shift in the way we treat CNS tumors. Rather than employing nonspecific therapies guided by crude measures of disease type, to treat the primary tumor mass, we should develop classification systems and targeted treatment strategies focusing on the eradication of cancer stem cells (Pardal et al., 2003). This strategy may prove particularly effective in tumors, such as ependymoma, that are comprised of developmentally and molecularly distinct subgroups that are unlikely to respond uniformly to all treatments.

One of the most immediate clinical applications of cancer stem cell biology is the generation of prognostic tools (Glinsky et al., 2005; Singh et al., 2003). However, there is a greater need for better treatments of ependymoma, since the survival of patients with partially resected ependymoma is extremely poor (Bouffet et al., 1998). At least two aspects of the biology of cancer stem cells could be exploited as new therapeutic targets. Stem cells are distinguished from their differentiated progeny by the expression of high levels of ATP binding cassette (ABC) transporters (Dean et al., 2005). These proteins are not required for stem cell growth or maintenance, but they likely serve a protective function that prevents stem cells from accumulating toxins (Schinkel et al., 1994; Zhou et al., 2002). Unfortunately, ABC transporters are also highly effective at excluding drugs from cells, and this may explain why normal and malignant stem cells are peculiarly resistant to certain chemo-

therapeutics (Dean et al., 2005). Interestingly, supratentorial ependymomas expressed significantly higher amounts of the ABC transporter ABCG1 relative to ependymomas elsewhere in the CNS (2.5-fold increase in expression; $p < 0.0005$; see Table S1). Thus, inhibitors of ABC transporters may prove to be useful therapeutics to increase the sensitivity of ependymoma cancer stem cells to conventional treatments (Dean et al., 2005).

Targeting the pathways that regulate aberrant self-renewal represents an alternative approach to attacking stem cells in cancer (Pardal et al., 2003). The success of this approach will depend on our ability to develop drugs that selectively target cancer stem cells while sparing their normal counterparts. This issue is especially important when treating brain tumors in children, whose nervous systems are still developing. The extent to which normal neural stem cells repair radiation-induced damage in the brain is not known. Thus, relatively nonselective drugs that target both normal and malignant stem cell fractions might compound the deleterious effects of radiation therapy. These issues aside, there is a real possibility that drugs that inhibit the self-renewal of cancer stem cells could offer new hope to patients with refractory malignancies such as ependymoma. Indeed, one class of drugs, inhibitors of γ-secretase, are being considered for clinical trials in leukemia and could have utility in the treatment of supratentorial ependymoma (Huntly and Gilliland, 2005). Binding of JAGGED ligands to NOTCH leads to γ-secretase-mediated cleavage of the NOTCH receptor and activation of signaling (Radtke and Raj, 2003). Thus, if JAGGED1 contributes to the stem cell phenotype in supratentorial tumors, then inhibitors of γ-secretase might be effective against these tumors.

The approach used here to identify ependymoma cancer stem cells and the corresponding normal progenitor cells could be readily adapted to the analysis of other organ systems. While cancer stem cells have been isolated from solid tumors of the brain and breast, the relationship of these cells to normal progenitors in the respective tissues of origin is unknown (Al-Hajj and Clarke, 2004; Singh et al., 2004a). We demonstrate that screening developing tissues for cells that exhibit the signature gene expression profiles of tumor subsets can identify progenitor cells that may represent the cellular targets of primary mutations that promote disease. Thus, molecular archeology studies of tumor stem cells could reveal the susceptible progenitor cell population that gives rise to many distinct cancer subtypes.

Experimental procedures

Patient samples

Clinical material was collected under protocol XPD01-092 (St. Jude Children's Research Hospital Institutional Review Board) and subject to central histopathology review. Tumor samples were snap frozen at the time of surgical resection or immediately disaggregated into single-cell suspensions and cultured as described below. A separate, nonoverlapping cohort of formalin-fixed, wax-embedded ependymoma samples were also collected and incorporated into a TMA. RNA and DNA were extracted from fresh-frozen tumor samples using Trizol as directed by the manufacturer and were stored at −80°C until use.

Oligonucleotide RNA expression array analysis

Gene expression profiles were generated using total RNA and the U133Av2 array (Affymetrix) that analyzes the expression level of 18,400 transcripts and variants, including 14,500 well-characterized human genes (Hernan et al., 2003). Gene expression data were normalized using the MAS5 algorithm and then transformed by taking the logarithm (base 2) and the coefficient of variation (CV) calculated for each probe set across all samples. The top 1000 most variable probe sets were selected for unsupervised hierarchical clustering based on Z scores using Pearson correlation as the similarity metric.

We used analysis of variance (ANOVA) to identify probe sets that discriminated tumor subtypes. To correct for the multiple hypothesis testing problem, false discovery rates (q values) were calculated from the ANOVA p values (Storey and Tibshirani, 2003). Probe sets with q values less than 0.05 were then filtered further to remove probe sets with intergroup fold changes of less than 1.5. Selected probe sets were then used for supervised hierarchical clustering.

aCGH

Total genomic DNA from test samples and sex-matched reference DNA samples were processed and analyzed using BAC array CGH exactly as described previously (Loo et al., 2004). For a full description of this array, the reader is referred to Loo et al. (2004). Briefly, this array includes 4171 different BAC clones with a median spacing of 413 kb when pericentric heterochromatic regions and the short arms of acrocentric chromosomes are excluded (25th percentile, 160 kb; 75th percentile, 878 kb; mean, 677 kb). The locations of 4153 clones have been verified by FISH.

We performed a global within-slide normalization to remove intensity-dependent bias using the robust scatter plot smoother "*loess*" and then performed a multiple slide scale normalization to facilitate between-slide comparisons using the median absolute deviation (MAD) with Bioconductor version 1.5. An average ratio was then calculated for each BAC clone, since each BAC clone was spotted twice per microarray.

Thresholds reporting chromosome gains or losses for each BAC were calculated using the extreme studentized deviate (ESD) statistic:

$$\text{ESD} = \text{maximum of } Z_{i=1,\ldots,n} = |X_i - \bar{X}| / S$$

where $X_1, \ldots, X_n$ denote the ratios across samples, and $\bar{X}$ and S denote the mean and standard deviation for sample ratios for a specific BAC clone. This approach assumes that ratios from samples without DNA copy number changes follow a Gaussian distribution for a specific BAC clone and that ratios from samples with DNA copy number changes are outliers relative to Gaussian distribution for same BAC clone. We then used an established ESD-based procedure to detect outliers. BAC clones that had either gain or loss at more than or equal to three samples were then selected for unsupervised hierarchical clustering using Euclidean distance as a similarity metric.

To evaluate the influence of DNA copy number changes on gene expression, we identified all Affymetrix probe sets that mapped within significantly varying BAC aCGH clones. aCGH data were represented by a vector that was labeled 1 for a sample with DNA copy number change and 0 for no change. DNA copy number changes were then correlated with gene expression using the *t*-like statistic defined as the difference of the means of the gene expression values in the altered and unaltered sample groups divided by the sum of the standard deviations of the expression values in altered and unaltered sample groups. To assess the significance of each statistic for each gene, we performed random permutations of the label vector of samples. The probability that a gene has a larger or equal statistic by random permutation than the original statistic is denoted by α. A low α (<0.05) indicates a strong association between gene expression and DNA copy number changes.

In situ hybridization analysis

Cryosections (16 μm) were prepared from 4% paraformaldehyde (PFA)-fixed whole brains and spinal cord taken from E11.5, E15.5, and postnatal day 7 (P7) C57BL/6 mice. ^{33}P-UTP riboprobes were generated by in vitro transcription. Following incubation with 1×10^6 cpm of probe, slides were rinsed through a series of posthybridization washes, air-dried, and exposed to emulsion.

Cell culture and orthotopic transplants

Immediately following surgical resection, tumors were minced and digested with collagenase type IV and hyaluronidase for 60 min at 37°C. Cells were then grown on Matrigel (BD BioSciences)-coated dishes in Neurobasal medium (Invitrogen) containing 2 mM L-glutamine, N2 supplement (Invitrogen),

B27 supplement (Invitrogen), 20 ng/ml hrEGF (Invitrogen), 20 ng/ml hrbFGF (Invitrogen) and 50 μg/ml BSA in 5% CO_2. Serial dilutions of single-cell suspensions were made in 96 well plates. The number of tumor spheres/well was quantified after 7 days. For differentiation studies, tumor spheres were transferred to culture slides coated with poly-L-ornithine and laminin and incubated in Neurobasal medium without growth factors for 72 hr. All cell cultures were subject to spectral karyotype analysis to confirm the presence of malignant clones.

Human ependymoma cells were sorted using antibody coated magnetic beads (100μl/10^8 cells, Miltenyi Biotec). Sorted cells were resuspended in Matrigel (5 μl; BD BioScience) and implanted intracranially into 7- to 8-week-old NOD/SCID mice at a depth of 3.5 mm. Purity of the sorted cell populations was confirmed by immunocytochemistry using anti-CD133/2 (Miltenyi Biotec).

FISH and immunohistochemical analyses

Dual-color FISH and immunohistochemical analyses of formalin-fixed paraffin-embedded tumor samples or tumor cell spheres were performed using routine methods. Full details of all immunoreagents used in this study are provided in Table S5. All FISH probes were validated on normal control metaphase spreads to verify chromosomal localization.

Supplemental data

The Supplemental Data include five supplemental tables and can be found with this article online at http://www.cancercell.org/cgi/content/full/8/4/323/DC1/.

Acknowledgments

This work was supported by the Sontag Foundation (R.J.G.), NIH grant CA096832 (R.J.G.), the V Foundation for Cancer Research (R.J.G.), the American Lebanese Syrian Associated Charities (ALSAC), and a Detweiller Travelling Fellowship from the Royal College of Physicians and Surgeons of Canada (M.D.T.). We thank the Tumor Bank and Hartwell Center for Bioinformatics and Biotechnology at St. Jude Children's Research Hospital; the Brain Tumor Tissue Bank (London, Ontario, Canada) for outstanding technical assistance; and Betsy Williford in Biomedical Communications at St. Jude Children's Research Hospital for assistance in preparing the figures. The BLBP antibody was the generous gift of Nathaniel Heintz.

Received: June 13, 2005
Revised: August 1, 2005
Accepted: September 6, 2005
Published: October 17, 2005

References

Aguirre, A.J., Brennan, C., Bailey, G., Sinha, R., Feng, B., Leo, C., Zhang, Y., Zhang, J., Gans, J.D., Bardeesy, N., et al. (2004). High-resolution characterization of the pancreatic adenocarcinoma genome. Proc. Natl. Acad. Sci. USA *101*, 9067–9072.

Al-Hajj, M., and Clarke, M.F. (2004). Self-renewal and solid tumor stem cells. Oncogene *23*, 7274–7282.

Bonnet, D., and Dick, J.E. (1997). Human acute myeloid leukemia is organized as a hierarchy that originates from a primitive hematopoietic cell. Nat. Med. *3*, 730–737.

Bouffet, E., Perilongo, G., Canete, A., and Massimino, M. (1998). Intracranial ependymomas in children: a critical review of prognostic factors and a plea for cooperation. Med. Pediatr. Oncol. *30*, 319–329.

Capela, A., and Temple, S. (2002). LeX/ssea-1 is expressed by adult mouse CNS stem cells, identifying them as nonependymal. Neuron *35*, 865–875.

Castor, A., Nilsson, L., Astrand-Grundstrom, I., Buitenhuis, M., Ramirez, C., Anderson, K., Strombeck, B., Garwicz, S., Bekassy, A.N., Schmiegelow, K., et al. (2005). Distinct patterns of hematopoietic stem cell involvement in acute lymphoblastic leukemia. Nat. Med. *11*, 630–637. Published online May 22, 2005. 10.1038/nm1253.

Conover, J.C., Doetsch, F., Garcia-Verdugo, J.M., Gale, N.W., Yancopoulos, G.D., and Alvarez-Buylla, A. (2000). Disruption of Eph/ephrin signaling affects migration and proliferation in the adult subventricular zone. Nat. Neurosci. *3*, 1091–1097.

Culican, S.M., Baumrind, N.L., Yamamoto, M., and Pearlman, A.L. (1990). Cortical radial glia: identification in tissue culture and evidence for their transformation to astrocytes. J. Neurosci. *10*, 684–692.

Dasen, J.S., Liu, J.P., and Jessell, T.M. (2003). Motor neuron columnar fate imposed by sequential phases of Hox-c activity. Nature *425*, 926–933.

Dean, M., Fojo, T., and Bates, S. (2005). Tumour stem cells and drug resistance. Nat. Rev. Cancer *5*, 275–284.

Dyer, S., Prebble, E., Davison, V., Davies, P., Ramani, P., Ellison, D., and Grundy, R. (2002). Genomic imbalances in pediatric intracranial ependymomas define clinically relevant groups. Am. J. Pathol. *161*, 2133–2141.

Ebert, C., von Haken, M., Meyer-Puttlitz, B., Wiestler, O.D., Reifenberger, G., Pietsch, T., and von Deimling, A. (1999). Molecular genetic analysis of ependymal tumors. NF2 mutations and chromosome 22q loss occur preferentially in intramedullary spinal ependymomas. Am. J. Pathol. *155*, 627–632.

Fromental-Ramain, C., Warot, X., Lakkaraju, S., Favier, B., Haack, H., Birling, C., Dierich, A., Dollé, P., and Chambon, P. (1996). Specific and redundant functions of the paralogous Hoxa-9 and Hoxd-9 genes in forelimb and axial skeleton patterning. Development *122*, 461–472.

Glinsky, G.V., Berezovska, O., and Glinskii, A.B. (2005). Microarray analysis identifies a death-from-cancer signature predicting therapy failure in patients with multiple types of cancer. J. Clin. Invest. *115*, 1503–1521.

Hartfuss, E., Galli, R., Heins, N., and Gotz, M. (2001). Characterization of CNS precursor subtypes and radial glia. Dev. Biol. *229*, 15–30.

Hemmati, H.D., Nakano, I., Lazareff, J.A., Masterman-Smith, M., Geschwind, D.H., Bronner-Fraser, M., and Kornblum, H.I. (2003). Cancerous stem cells can arise from pediatric brain tumors. Proc. Natl. Acad. Sci. USA *100*, 15178–15183. Published online November 26, 2003. 10.1073/pnas.2036535100.

Hernan, R., Fasheh, R., Calabrese, C., Frank, A.J., Maclean, K.H., Allard, D., Barraclough, R., and Gilbertson, R.J. (2003). ERBB2 up-regulates S100A4 and several other prometastatic genes in medulloblastoma. Cancer Res. *63*, 140–148.

Hitoshi, S., Alexson, T., Tropepe, V., Donoviel, D., Elia, A.J., Nye, J.S., Conlon, R.A., Mak, T.W., Bernstein, A., and van der Kooy, D. (2002). Notch pathway molecules are essential for the maintenance, but not the generation, of mammalian neural stem cells. Genes Dev. *16*, 846–858.

Huang, B., Starostik, P., Kuhl, J., Tonn, J.C., and Roggendorf, W. (2002). Loss of heterozygosity on chromosome 22 in human ependymomas. Acta Neuropathol. (Berl.) *103*, 415–420. Published online January 17, 2002. 10.1007/s00401-001-0479-3.

Huntly, B.J., and Gilliland, D.G. (2005). Leukaemia stem cells and the evolution of cancer-stem-cell research. Nat. Rev. Cancer *5*, 311–321.

Huntly, B.J., Shigematsu, H., Deguchi, K., Lee, B.H., Mizuno, S., Duclos, N., Rowan, R., Amaral, S., Curley, D., Williams, I.R., et al. (2004). MOZ-TIF2, but not BCR-ABL, confers properties of leukemic stem cells to committed murine hematopoietic progenitors. Cancer Cell *6*, 587–596.

Ignatova, T.N., Kukekov, V.G., Laywell, E.D., Suslov, O.N., Vrionis, F.D., and Steindler, D.A. (2002). Human cortical glial tumors contain neural stem-like cells expressing astroglial and neuronal markers in vitro. Glia *39*, 193–206.

Kleihues, P., Louis, D.N., Scheithauer, B.W., Rorke, L.B., Reifenberger, G., Burger, P.C., and Cavenee, W.K. (2002). The WHO classification of tumors of the nervous system. J. Neuropathol. Exp. Neurol. *61*, 215–225.

Kmita, M., and Duboule, D. (2003). Organizing axes in time and space; 25 years of colinear tinkering. Science *301*, 331–333.

Kriegstein, A.R., and Gotz, M. (2003). Radial glia diversity: a matter of cell fate. Glia *43*, 37–43.

Lapidot, T., Sirard, C., Vormoor, J., Murdoch, B., Hoang, T., Caceres-Cortes, J., Minden, M., Paterson, B., Caligiuri, M.A., and Dick, J.E. (1994). A cell

initiating human acute myeloid leukaemia after transplantation into SCID mice. Nature *367*, 645–648.

Laywell, E.D., Rakic, P., Kukekov, V.G., Holland, E.C., and Steindler, D.A. (2000). Identification of a multipotent astrocytic stem cell in the immature and adult mouse brain. Proc. Natl. Acad. Sci. USA *97*, 13883–13888.

Liberski, P.P. (1996). The ultrastructure of ependymoma: personal experience and the review of the literature. Folia Neuropathol. *34*, 212–220.

Loo, L.W., Grove, D.I., Williams, E.M., Neal, C.L., Cousens, L.A., Schubert, E.L., Holcomb, I.N., Massa, H.F., Glogovac, J., Li, C.I., et al. (2004). Array comparative genomic hybridization analysis of genomic alterations in breast cancer subtypes. Cancer Res. *64*, 8541–8549.

Malatesta, P., Hack, M.A., Hartfuss, E., Kettenmann, H., Klinkert, W., Kirchhoff, F., and Gotz, M. (2003). Neuronal or glial progeny: Regional differences in radial glia fate. Neuron *37*, 751–764.

McMahon, S.S., and McDermott, K.W. (2002). Morphology and differentiation of radial glia in the developing rat spinal cord. J. Comp. Neurol. *454*, 263–271.

Miyamoto, T., Weissman, I.L., and Akashi, K. (2000). AML1/ETO-expressing nonleukemic stem cells in acute myelogenous leukemia with 8;21 chromosomal translocation. Proc. Natl. Acad. Sci. USA *97*, 7521–7526.

Nutt, C.L., Mani, D.R., Betensky, R.A., Tamayo, P., Cairncross, J.G., Ladd, C., Pohl, U., Hartmann, C., McLaughlin, M.E., Batchelor, T.T., et al. (2003). Gene expression-based classification of malignant gliomas correlates better with survival than histological classification. Cancer Res. *63*, 1602–1607.

Pardal, R., Clarke, M.F., and Morrison, S.J. (2003). Applying the principles of stem-cell biology to cancer. Nat. Rev. Cancer *3*, 895–902.

Radtke, F., and Raj, K. (2003). The role of Notch in tumorigenesis: oncogene or tumour suppressor? Nat. Rev. Cancer *3*, 756–767.

Reynolds, B.A., and Weiss, S. (1992). Generation of neurons and astrocytes from isolated cells of the adult mammalian central nervous system. Science *255*, 1707–1710.

Ross, M.E., Mahfouz, R., Onciu, M., Liu, H.C., Zhou, X., Song, G., Shurtleff, S.A., Pounds, S., Cheng, C., Ma, J., et al. (2004). Gene expression profiling of pediatric acute myelogenous leukemia. Blood *104*, 3679–3687. Published online June 29, 2004. 10.1182/blood-2004-03-1154.

Russo, R.E., Fernandez, A., Reali, C., Radmilovich, M., and Trujillo-Cenoz, O. (2004). Functional and molecular clues reveal precursor-like cells and immature neurones in the turtle spinal cord. J. Physiol. *560*, 831–838. Published online August 26, 2004. 10.1113/jphysiol.2004.072405.

Schinkel, A.H., Smit, J.J., van Tellingen, O., Beijnen, J.H., Wagenaar, E., van Deemter, L., Mol, C.A., van der Valk, M.A., Robanus-Maandag, E.C., te Riele, H.P., et al. (1994). Disruption of the mouse mdr1a P-glycoprotein gene leads to a deficiency in the blood-brain barrier and to increased sensitivity to drugs. Cell *77*, 491–502.

Singh, S.K., Clarke, I.D., Terasaki, M., Bonn, V.E., Hawkins, C., Squire, J., and Dirks, P.B. (2003). Identification of a cancer stem cell in human brain tumors. Cancer Res. *63*, 5821–5828.

Singh, S.K., Clarke, I.D., Hide, T., and Dirks, P.B. (2004a). Cancer stem cells in nervous system tumors. Oncogene *23*, 7267–7273.

Singh, S.K., Hawkins, C., Clarke, I.D., Squire, J.A., Bayani, J., Hide, T., Henkelman, R.M., Cusimano, M.D., and Dirks, P.B. (2004b). Identification of human brain tumour initiating cells. Nature *432*, 396–401.

Sotiriou, C., Neo, S.Y., McShane, L.M., Korn, E.L., Long, P.M., Jazaeri, A., Martiat, P., Fox, S.B., Harris, A.L., and Liu, E.T. (2003). Breast cancer classification and prognosis based on gene expression profiles from a population-based study. Proc. Natl. Acad. Sci. USA *100*, 10393–10398. Published online August 13, 2003. 10.1073/pnas.1732912100.

Spassky, N., Merkle, F.T., Flames, N., Tramontin, A.D., Garcia-Verdugo, J.M., and Alvarez-Buylla, A. (2005). Adult ependymal cells are postmitotic and are derived from radial glial cells during embryogenesis. J. Neurosci. *25*, 10–18.

Storey, J.D., and Tibshirani, R. (2003). Statistical significance for genomewide studies. Proc. Natl. Acad. Sci. USA *100*, 9440–9445. Published online July 25, 2003. 10.1073/pnas.1530509100.

Suarez-Merino, B., Hubank, M., Revesz, T., Harkness, W., Hayward, R., Thompson, D., Darling, J.L., Thomas, D.G., and Warr, T.J. (2005). Microarray analysis of pediatric ependymoma identifies a cluster of 112 candidate genes including four transcripts at 22q12.1-q13.3. Neuro-oncol. *7*, 20–31.

Suemori, H., and Noguchi, S. (2000). Hox C cluster genes are dispensable for overall body plan of mouse embryonic development. Dev. Biol. *220*, 333–342.

Uchida, N., Buck, D.W., He, D., Reitsma, M.J., Masek, M., Phan, T.V., Tsukamoto, A.S., Gage, F.H., and Weissman, I.L. (2000). Direct isolation of human central nervous system stem cells. Proc. Natl. Acad. Sci. USA *97*, 14720–14725.

Varnum-Finney, B., Purton, L.E., Yu, M., Brashem-Stein, C., Flowers, D., Staats, S., Moore, K.A., Le Roux, I., Mann, R., Gray, G., et al. (1998). The Notch ligand, Jagged-1, influences the development of primitive hematopoietic precursor cells. Blood *91*, 4084–4091.

Warner, J.K., Wang, J.C., Hope, K.J., Jin, L., and Dick, J.E. (2004). Concepts of human leukemic development. Oncogene *23*, 7164–7177.

Yeoh, E.J., Ross, M.E., Shurtleff, S.A., Williams, W.K., Patel, D., Mahfouz, R., Behm, F.G., Raimondi, S.C., Relling, M.V., Patel, A., et al. (2002). Classification, subtype discovery, and prediction of outcome in pediatric acute lymphoblastic leukemia by gene expression profiling. Cancer Cell *1*, 133–143.

Yuan, Y., Zhou, L., Miyamoto, T., Iwasaki, H., Harakawa, N., Hetherington, C.J., Burel, S.A., Lagasse, E., Weissman, I.L., Akashi, K., and Zhang, D.E. (2001). AML1-ETO expression is directly involved in the development of acute myeloid leukemia in the presence of additional mutations. Proc. Natl. Acad. Sci. USA *98*, 10398–10403.

Yuan, X., Curtin, J., Xiong, Y., Liu, G., Waschsmann-Hogiu, S., Farkas, D.L., Black, K.L., and Yu, J.S. (2004). Isolation of cancer stem cells from adult glioblastoma multiforme. Oncogene *23*, 9392–9400.

Zhou, S., Morris, J.J., Barnes, Y., Lan, L., Schuetz, J.D., and Sorrentino, B.P. (2002). Bcrp1 gene expression is required for normal numbers of side population stem cells in mice, and confers relative protection to mitoxantrone in hematopoietic cells in vivo. Proc. Natl. Acad. Sci. USA *99*, 12339–12344. Published online September 6, 2002. 10.1073/pnas.192276999.